Mathematics

AIMS Mathematics, 11(8): 25984–26005.
DOI: 10.3934/math.20261041
Received: 14 April 2026
Revised: 10 July 2026
Accepted: 31 July 2026
Published: 20 August 2026

https://www.aimspress.com/journal/Math

Research article

Composite finite-time attitude tracking control for Quadrotor UAVs with prescribed performance constraints

Huawei Niu[1,2], Qixun Lan[3,*], Xuehai Wang[2] and Jingjing Mu[4]

[1] School of Mathematics, Pingdingshan Vocational and Technical College, Pingdingshan 467000, China
[2] School of Mathematics and Statistics, Xinyang Normal University, Xinyang 464000, China
[3] College of Electrical and Information Engineering, Zhengzhou University of Light Industry, Zhengzhou 450002, China
[4] School of Mathematical Sciences, Henan University of Urban College, Pingdingshan 467036, China

* **Correspondence:** Email: q.lan@zzuli.edu.cn.

Abstract: In this paper, we address the finite-time attitude tracking control problem for quadrotor unmanned aerial vehicles (UAVs) subject to external disturbances and prescribed state constraints. A novel composite control framework was proposed, which integrated a finite-time disturbance observer (FTDO) with a barrier Lyapunov function (BLF)-based homogeneous controller. Specifically, an FTDO was first designed to achieve rapid and accurate estimation of the lumped disturbance, which encompassed external disturbances and model uncertainties. Then, a tangent-type barrier Lyapunov function (BLF) was constructed to prevent violation of the prescribed state constraints. Subsequently, a tangent-type BLF was introduced to strictly enforce the predefined attitude constraints. By leveraging homogeneous system theory and incorporating the disturbance estimates for feedforward compensation, a continuous composite finite-time controller was synthesized. Rigorous Lyapunov analysis demonstrated that under the proposed scheme, all closed-loop signals remained bounded, and the attitude tracking errors converged to zero within finite time, and the prescribed state constraints were never transgressed. Simulation results demonstrated the effectiveness of the proposed control scheme.

Keywords: quadrotor UAV; prescribed state constraints; disturbance observer; finite-time control; barrier Lyapunov function
Mathematics Subject Classification: 93B12, 93C85, 93D40

1. Introduction

Quadrotor unmanned aerial vehicles (UAVs) have found widespread applications in military reconnaissance, logistics transportation, and aerial surveillance [1,2], owing to their mechanical simplicity, agile maneuverability, and vertical take-off and landing (VTOL) capability. Their modular architecture further facilitates efficient deployment in large-scale scenarios, such as agricultural monitoring and infrastructure inspection. However, in mission-critical tasks demanding high dynamic performance such as formation flight and precision payload delivery the attitude control system must ensure not only robustness against external disturbances but also strict adherence to predefined state constraints (e.g., angular velocity or attitude angle limits) [3]. Violation of these constraints can lead to performance degradation or instability. Moreover, the convergence speed of attitude tracking is often required to be finite-time to meet the stringent temporal demands of agile maneuvers [4]. Satisfying these simultaneous requirements of disturbance rejection, constraint satisfaction, and finite-time convergence poses a significant and open challenge for controller design.

A substantial body of research has been devoted to attitude control of quadrotor UAVs. Linear methods, such as PID and linear quadratic regulators (LQR), offer simple structures but exhibit limited robustness against strong nonlinearities and external disturbances [5]. To address system nonlinearities, nonlinear control techniques including feedback linearization [6], backstepping [7], and sliding mode control (SMC) [8,9] have been proposed, achieving improved performance. Nevertheless, these methods primarily rely on the controller's inherent robustness to suppress disturbances. As a step toward more proactive uncertainty compensation, adaptive fuzzy switching tracking algorithms have been developed for flexible robotic systems [10]. To more proactively reject disturbances, observer-based active anti-disturbance control has gained prominence [11]. Strategies such as disturbance observer-based control (DOBC) [12,13], active disturbance rejection control (ADRC) [14], and finite-time disturbance observers (FTDO) [15] enable real-time estimation and feedforward compensation of lumped disturbances, significantly enhancing system robustness.

While effective in disturbance rejection, the aforementioned methods share two common limitations. First, they lack a systematic mechanism to explicitly handle state constraints. Although barrier Lyapunov functions (BLFs) have been introduced to prevent constraint violations [16,17], conventional BLF-based designs typically achieve only asymptotic stability. Second, the convergence rate of tracking errors in these frameworks is often at best exponential, which may not suffice for applications requiring finite-time convergence. Some researchers have explored finite-time control techniques [18] or BLF-based constrained control [19] in isolation, but the simultaneous consideration of lumped disturbances, prescribed state constraints, and finite-time convergence remains an unresolved problem. It is worth noting that while related challenges in stochastic nonlinear systems have been addressed via designated-time stabilization [20], such approaches do not directly translate to the deterministic, disturbance-prone, and tightly constrained attitude tracking problem of quadrotor UAVs considered herein. Moreover, quadrotor control with prescribed performance and prescribed-time convergence has drawn increasing attention. The researchers in [21] proposed a prescribed-performance tracking scheme with prescribed-time guarantees under arbitrary initial conditions. Tian et al. [22] developed a fault-tolerant prescribed-time controller with guaranteed performance, while Wang et al. [23] presented a prescribed finite-time attitude tracking method. Zhang et al. [24] investigated anti-saturation fast super-twisting sliding mode control, and Vutukuri and Padhi [25] addressed predefined-time prescribed performance control for spacecraft, whose framework is methodologically transferable to quadrotor systems. However, these approaches treat prescribed performance and convergence-time specification as separate objectives, and none simultaneously ensures lumped disturbance rejection, strict constraint satisfaction, and finite-time convergence within a unified framework.

Motivated by this gap, we propose a novel composite control framework for quadrotor UAV attitude tracking subject to external disturbances and prescribed state constraints. The proposed scheme integrates a FTDO with a tangent-type barrier Lyapunov function (BLF)-based homogeneous controller. The major contributions are summarized as follows:

(i) A finite-time disturbance observer is designed to achieve rapid and exact estimation of lumped disturbances, enabling effective feedforward compensation.

(ii) A tangent-type BLF is constructed to strictly enforce predefined attitude constraints, ensuring never violation during operation.

(iii) By leveraging homogeneous system theory, a continuous composite finite-time controller is synthesized, guaranteeing that attitude tracking errors converge to zero within finite time while maintaining all closed-loop signals bounded. Rigorous Lyapunov analysis and simulation studies validate the efficacy of the proposed scheme.

(iv) Unlike constrained control schemes that only ensure asymptotic stability (e.g., CFO-BLF in [26]), the proposed strategy guarantees finite-time convergence of attitude tracking errors. Comparative simulations in Section 4.2.3, evaluating tracking accuracy, convergence speed, constraint satisfaction, and control smoothness, demonstrate the significant improvements of the proposed scheme in transient and steady-state performances.

2. Quadrotor UAV system modeling

2.1. Problem formulation

A quadrotor UAV achieves attitude and position control by adjusting the rotational speeds of its four rotors. The simplified structure is shown in Figure 1. To describe its motion, we define an earth-fixed inertial frame [27] $(O_e: X_e\, Y_e\, Z_e)$and a body-fixed frame $(o_b: x_b\, y_b\, z_b)$. The orientation of the body frame relative to the inertial frame is represented by Euler angles: The roll angle φ (rotation about the $o_b x_b$-axis), pitch angle θ (rotation about the $o_b y_b$-axis), and yaw angle ψ (rotation about the $o_b z_b$-axis). The corresponding angular velocities are denoted as ω_x, ω_y, and ω_z, respectively.

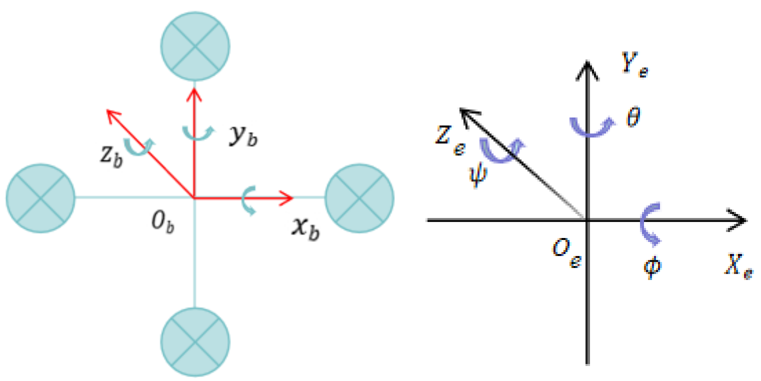

Figure 1. Schematic diagram of the quadrotor UAV structure.

We assume that the rotational speeds of the four rotors are ω_1、ω_2、ω_3 and ω_4, respectively. The total lift force generated along the $o_b z_b$ axis is denoted as u_L, and the torques about three body axis are denoted as τ_φ, τ_θ, and τ_ψ. Based on the symmetric configuration of the quadrotor and the associated aerodynamic relationships, the resultant forces and moments can be expressed as follows:

$$
\begin{cases}
u_L = k(\omega_1^2 + \omega_2^2 + \omega_3^2 + \omega_4^2), \\
\tau_\varphi = lk(\omega_2^2 - \omega_4^2), \\
\tau_\theta = lk(-\omega_1^2 + \omega_3^2), \\
\tau_\psi = b(-\omega_1^2 + \omega_2^2 - \omega_3^2 + \omega_4^2),
\end{cases}
\tag{2.1}
$$

where k denotes the thrust coefficient, l represents the arm length from the rotor center to the UAV's center of mass, and b is the torque coefficient.

2.2. Attitude dynamics model

Employing the Newton-Euler formulation [28, 29], the attitude dynamics of a quadrotor UAV in the presence of external disturbances can be described as follows:

$$
\begin{cases}
\dot{\varphi} = p + q \sin\varphi \tan\theta + r\cos\varphi \tan\theta, \\
\dot{\theta} = q \cos\varphi - r \sin\varphi, \\
\dot{\psi} = q\frac{\sin\varphi}{\cos\theta} + r\frac{\cos\varphi}{\cos\theta}, \\
\dot{p} = \frac{I_y - I_z}{I_x} qr + \frac{1}{I_x}\tau_\varphi + \frac{1}{I_x}\tau_{d\varphi}, \\
\dot{q} = \frac{I_z - I_x}{I_y} pr + \frac{1}{I_y}\tau_\theta + \frac{1}{I_y}\tau_{d\theta}, \\
\dot{r} = \frac{I_x - I_y}{I_z} pq + \frac{1}{I_z}\tau_\psi + \frac{1}{I_z}\tau_{d\psi},
\end{cases}
\tag{2.2}
$$

where p, q, r denotes the angular velocity of the rigid body; I_x, I_y, I_z are the moment of inertia; τ_φ, τ_θ and τ_ψ stands for the control torque; $\tau_{d\varphi}$, $\tau_{d\theta}$ and $\tau_{d\psi}$ represent the external disturbance torques.

To facilitate subsequent analysis and controller design, the system in (2.2) can be rewritten in the following concise form:

$$
\begin{cases}
\dot{\Theta} = W\Omega, \\
\dot{\Omega} = -I^{-1}(\Omega_\times I\Omega) + I^{-1}\tau_u + I^{-1}\tau_d,
\end{cases}
\tag{2.3}
$$

where

$$
\Theta = \begin{bmatrix} \varphi \\ \theta \\ \psi \end{bmatrix},\ \Omega = \begin{bmatrix} p \\ q \\ r \end{bmatrix},\ I = \begin{bmatrix} I_x & 0 & 0 \\ 0 & I_y & 0 \\ 0 & 0 & I_z \end{bmatrix},\ \tau_u = \begin{bmatrix} \tau_\varphi \\ \tau_\theta \\ \tau_\psi \end{bmatrix},\ \tau_d = \begin{bmatrix} \tau_{d\varphi} \\ \tau_{d\theta} \\ \tau_{d\psi} \end{bmatrix},
$$

$$
\Omega_\times = \begin{bmatrix} 0 & -r & q \\ r & 0 & -p \\ -q & p & 0 \end{bmatrix},\ W = \begin{bmatrix} 1 & \sin\varphi \tan\theta & \cot\varphi \tan\theta \\ 0 & \cot\varphi & -\sin\varphi \\ 0 & \sin\varphi / \cos\theta & \cos\varphi / \cos\theta \end{bmatrix}.
$$

I is the inertia matrix (considered diagonal and positive definite), τ_u is the control torque vector, τ_d is the lumped disturbance torque vector, and $\Omega_\times$ is the skew-symmetric matrix associated with the angular velocity, W is the attitude kinematics matrix.

The primary control objective is to track desired attitude angles φ^q, θ^q and ψ^q for the roll pitch and yaw channels, respectively. Since the actual control inputs are the rotational speeds of the four rotors ω_1, ω_2, ω_3 and ω_4 the moment allocation relationship given by (2.1) is not uniquely invertible. To address this issue, it is commonly assumed that under hovering conditions or when the small-angle approximation holds, the total lift u_L balances gravity:

$$u_L \cos\varphi \cos\theta = mg, \tag{2.4}$$

where m is the mass of UAV and g is the gravitational acceleration.

2.3. Decoupling of the attitude error dynamics

Kinematic coupling inherent in the attitude dynamics can induce undesired interactions that complicate controller design. To address this issue, we adopt a transformation to decouple the original dynamics into three independent channels, thereby facilitating the design of dedicated controllers for the roll, pitch, yaw axes and enhancing robustness against external disturbances to ensure flight stability in complex environments [16]. Define the attitude tracking error vector as:

$$e_\Theta = \Theta - \Theta^q = \begin{bmatrix} \varphi - \varphi^q \\ \theta - \theta^q \\ \psi - \psi^q \end{bmatrix} = \begin{bmatrix} e_\varphi \\ e_\theta \\ e_\psi \end{bmatrix}, \tag{2.5}$$

where $\Theta^q = [\varphi^q \quad \theta^q \quad \psi^q]^T$ is the desired attitude angle vector. Combining (2.3) with (2.5), the dynamics of the tracking error are derived as follows:

$$\begin{cases} \dot{e}_\Theta = W\Omega - \dot{\Theta}^q, \\ \ddot{e}_\Theta = -WI^{-1}(\Omega_\times I\Omega) + \dot{W}\Omega + WI^{-1}\tau_u + WI^{-1}\tau_d - \ddot{\Theta}^q, \end{cases} \tag{2.6}$$

where $\dot{\Theta}^q$ and $\ddot{\Theta}^q$ are the first and second derivatives of the desired attitude, respectively.

To facilitate controller design, the known dynamics and the equivalent control input are defined as follows:

$$f = -WI^{-1}(\Omega_\times I\Omega) + \dot{W}\Omega, \tau = WI^{-1}\tau_u, d = WI^{-1}\tau_d - \ddot{\Theta}^q,$$

where $f = [f_1 \quad f_2 \quad f_3]^T$ represents the known nonlinear terms, $\tau = [\tau_1 \quad \tau_2 \quad \tau_3]^T$ denotes the equivalent control inputs in the decoupled space, and $d = [d_1 \quad d_2 \quad d_3]^T$ stands for the lumped disturbance, which encompasses external disturbance torques and the feed forward terms associated with the desired trajectory.

Consequently, the attitude tracking error system (2.6) can be decoupled into three independent channels:

$$\begin{cases} \ddot{e}_\varphi = \tau_1 + f_1 + d_1, \\ \ddot{e}_\theta = \tau_2 + f_2 + d_2, \\ \ddot{e}_\psi = \tau_3 + f_3 + d_3. \end{cases} \tag{2.7}$$

Assumption 2.1. The lumped disturbance $d_i (i = 1,\ 2,\ 3)$ has bounded derivatives up to order $n-1$, and there exists a function $\eta_i(\cdot): R^{n-1} \to R$ such that

$$d_i^{(n-1)} = \eta_i\left(d_i, d_i^{(1)}, \cdots, d_i^{(n-2)}\right).$$

Through the above transformation, the original three-channel attitude tracking problem for the quadrotor UAV is converted into a stabilization problem for the error subsystems given in (2.7).

Remark 2.1. The desired tracking signals φ^q, θ^q, ψ^q are known a priori. However, their higher-order derivatives are often difficult to obtain directly in practice. Therefore, in Eq (2.6), the term $\ddot{\Theta}^q$ is incorporated into the lumped disturbance$d$for unified handling.

3. Results

3.1. Design of finite-time disturbance observer

Inspired by the finite-time disturbance observers proposed in [30,31], a finite-time disturbance observer (FTDO) is designed for system (2.7) to estimate $d(t)$ within a finite time. Define $z_{i1} = \dot{e}_i$, $z_{i,j+1} = d_i^{(j)}, i = 1, 2, 3, j = 1, \cdots, n-1$. With these definitions, system (2.7) can be reformulated as:

$$\begin{cases} \dot{z}_{i1} = \tau_i + f_i + z_{i2}, \\ \dot{z}_{ij} = z_{i,j+1}, j = 2, \cdots, n-1, \\ \dot{z}_{in} = \eta_i(z_{i2}, \cdots, z_{i,n-1}). \end{cases} \tag{3.1}$$

Since the system (2.7) is equivalent to the system (3.1), the design of a finite-time disturbance observer for (2.7) reduces to the design of a finite-time state observer for (3.1).

Lemma 3.1. For any ratio of odd even integers $\gamma \in (-1/n, 1)$, there exist positive constants k_i such that the system

$$\begin{cases} \dot{\varepsilon}_i = \varepsilon_{i+1} + k_i \varepsilon_1^{r_{i+1}}, i = 1, \cdots, n-1, \\ \dot{\varepsilon}_n = -k_n \varepsilon_1^{r_{n+1}}, \end{cases}$$

is globally finite-time stabile, where the exponents are defined recursively as $r_1 = 1,\ r_{i+1} = r_i + \gamma$, $i = 1,\ \cdots,\ n$.

Based on Lemma 3.1, a finite-time state observer for system (3.1) can be designed. The proof of which can be found in [32], and its properties are summarized in the following theorem.

Remark 3.1. Lemma 3.1 is employed to guarantee the finite-time convergence of the proposed FTDO. Specifically, it provides the theoretical foundation for constructing a set of auxiliary state variables and recursively defined exponents such that the observer dynamics become globally finite-time stable. This lemma ensures that the estimation errors, as defined in (3.4), converge to zero within a finite time, there by providing a theoretical guarantee for accurate disturbance feedforward compensation in the subsequent controller design.

Theorem 3.1. Consider system (3.1) with Assumption 2.1. There exists a constant $L \geq 1$ such that under the following observer

$$\begin{cases} \dot{\hat{z}}_{i1} = \hat{z}_{i2} + \tau_i + f_i + Lk_{i1}\varepsilon_1^{r_{i2}}, \\ \dot{\hat{z}}_{ij} = z_{i,j+1} + Lk_{ij}\varepsilon_1^{r_{i,j+1}}, j = 2, \cdots, n-1, \\ \dot{\hat{z}}_{in} = \hat{\eta}_i(\hat{z}_{i,2}, \cdots, \hat{z}_{i,n-1}) + L_n k_{i,n}\varepsilon_1^{r_{i,n+1}}, \end{cases}$$

estimates the states $(z_1, \cdots, z_n)$ of system (3.1) in finite time. The nonlinear function$\eta$is implemented with saturation to ensure boundedness, $\hat{\eta}(\hat{z}_2, \cdots, \hat{z}_n) = \eta(sat_B(\hat{z}_2), \cdots, (\hat{z}_n))$, with $B \geq b$, and the saturation function is defined as $sta_B(\hat{z}_i) = B \cdot sta(\hat{z}_i/B)$. The constants k_i and r_i are defined as in Lemma 3.1. The proof of this theorem can be found in [28].

To estimate the lumped disturbances d_1, d_2 and d_3 in the attitude loop, the following finite-time disturbance observers are designed based on the structure given in Theorem 3.1,

$$\begin{cases} \dot{z}_{i1} = \tau_i + f_i + d_i, \hat{d}_i = z_{i3}, i = 1, 2, 3, \\ \dot{z}_{i2} = \tau_i + f_i + z_{i3} + Lk_{i1}|z_{i1} - z_{i2}|^{r_{12}} sign(z_{i1} - z_{i2}), \\ \dot{z}_{i3} = z_{i4} + L^2 k_{i2}|z_{i1} - z_{i2}|^{r_{13}} sign(z_{i1} - z_{i2}), \\ \dot{z}_{i4} = z_{i5} + L^3 k_{i3}|z_{i1} - z_{i2}|^{r_{14}} sign(z_{i1} - z_{i2}), \\ \dot{z}_{i5} = -Sta_B(z_{i4}) + L^4 k_{i4}|z_{i1} - z_{i2}|^{r_{15}} sign(z_{i1} - z_{i2}), \end{cases} \tag{3.2}$$

where $\hat{d}_i$ denote the estimated values of the lumped disturbances, whose dynamics are governed by the system (2.7). The constants $k_{i1}, k_{i2}, k_{i3}, k_{i4}, L$ are observer gains and $r_i = 1 + (i-1)\gamma, \gamma \in (-\frac{1}{n}, 0)$ for $i = 2, \cdots, 5$.

Define the estimation errors of the finite-time sliding mode observer (3.2) as follows:

$$\begin{cases} e_1 = \hat{d}_1 - d_1, \\ e_2 = \hat{d}_2 - d_2, \\ e_3 = \hat{d}_3 - d_3. \end{cases} \tag{3.3}$$

Since the lumped disturbances satisfy system (2.7), it follows from the theorem presented in [33] that the observer estimation errors e_1, e_2, e_3 converge to zero during a finite time. Observing the system in (2.7) and the finite-time disturbance observers (3.2), it is evident that the dynamic models and observer designs for the roll, pitch, and yaw channels are structurally similar. Therefore, without loss of generality, the stability analysis in the following section is carried out for the pitch channel; the proofs for the remaining channels follow accordingly.

Remark 3.2. Finite-time observer design has been explored in several studies [18,31,34]. Unlike these works, which primarily focus on disturbance estimation for individual systems, our contribution lies in developing an FTDO framework rooted in a system-reconstruction philosophy. This framework not only achieves accurate finite-time estimation of lumped disturbances, but more importantly, is inherently compatible with a barrier Lyapunov function-based controller, enabling the unified resolution of three critical challenges in quadrotor attitude tracking—prescribed state constraints, mismatched disturbance rejection, and finite-time convergence—within a single coherent architecture. Furthermore, the proposed FTDO framework incorporates a complementary smoothing mechanism: The saturation-constrained implementation of the nonlinear function, which prevents unbounded growth of observer states during transients and limits the amplitude of high-frequency components.

3.2. Finite-time state feedback controller design based on FTDO

Define the attitude angle tracking error vector as defined in (2.5) and the output constraint be prescribed as $-\underline{c}_\theta \le e_\Theta \le \bar{c}_\theta$.

To handle this output constraint, a barrier Lyapunov function (BLF) is constructed. Taking the pitch channel as an illustrative example, let $D \in D_{(-\underline{c}_\theta, \bar{c}_\theta)} \to R$. The BLF is defined as follows:

$$V_b(e_\theta) = \frac{\bar{c}_\theta^{\left(\frac{r_3}{r_1}+1\right)} \underline{c}_\theta^{\left(\frac{r_3}{r_1}+1\right)} |e_\theta|^{\left(\frac{r_3}{r_1}+1\right)}}{\left(\frac{r_3}{r_1}+1\right)(\bar{c}_\theta - e_\theta)^{\left(\frac{r_3}{r_1}+1\right)} (\underline{c}_\theta + e_\theta)^{\left(\frac{r_3}{r_1}+1\right)}}, \tag{3.4}$$

where $r_1 = 1,\ r_i = r_{i-1} + \gamma$ for $i = 1, 2, 3$ and $\gamma \in (-\frac{1}{n}, 0)$.

It can be verified that $V_b(e_\theta)$ is positive definite and continuously differentiable. The partial derivative of $V_b(e_\theta)$ with respect to e_θ is given by:

$$\frac{\partial V_b(e_\theta)}{\partial e_\theta} = \lambda(e_\theta)[e_\theta]^{\frac{r_3}{r_1}},$$

where

$$\lambda(e_\theta) = \frac{\bar{c}_\theta^{\left(\frac{r_3}{r_1}+1\right)} \underline{c}_\theta^{\left(\frac{r_3}{r_1}+1\right)} (e_\theta^2 + \bar{c}_\theta \underline{c}_\theta)}{(\bar{c}_\theta - e_\theta)^{\left(\frac{r_3}{r_1}+2\right)} (\underline{c}_\theta + e_\theta)^{\left(\frac{r_3}{r_1}+2\right)}}.$$

Since the full state of the attitude system is measurable, a continuous finite-time sliding mode controller is proposed based on the BLF (3.4) and the disturbance estimates from the FTDO:

$$\ddot{e} = -l_{p1}\lambda(e_\theta)[e_\theta]^{\frac{r_3}{r_1}} - l_{d1}[\dot{e}_\theta]^{\frac{r_3}{r_2}} - (\hat{d} - d), \tag{3.5}$$

where l_{p1} and l_{d1} are positive definite constants. Given $\hat{d} - d = e_d$, (3.5) can be rewritten as:

$$\ddot{e} = -l_{p1}\lambda(e_\theta)[e_\theta]^{\frac{r_3}{r_1}} - l_{d1}[\dot{e}_\theta]^{\frac{r_3}{r_2}} - e_d. \tag{3.6}$$

Disturbance d is precisely estimated in finite time, i.e., $e_d \equiv 0$. After a finite-time instant, system (3.6) reduces to:

$$\ddot{e} = -l_{p1}\lambda(e_\theta)[e_\theta]^{\frac{r_3}{r_1}} - l_{d1}[\dot{e}_\theta]^{\frac{r_3}{r_2}}. \tag{3.7}$$

Under Assumption 2.1, the control laws for the three channels can be designed symmetrically as follows:

$$\begin{cases} \tau_1 = -l_{p1}\lambda(e_\varphi)[e_\varphi]^{\frac{r_3}{r_1}} - l_{d1}[\dot{e}_\varphi]^{\frac{r_3}{r_2}} - f_1 - \hat{d}_1, \\ \tau_2 = -l_{p2}\lambda(e_\theta)[e_\theta]^{\frac{r_3}{r_1}} - l_{d2}[\dot{e}_\theta]^{\frac{r_3}{r_2}} - f_2 - \hat{d}_2, \\ \tau_3 = -l_{p3}\lambda(e_\phi)[e_\phi]^{\frac{r_3}{r_1}} - l_{d3}[\dot{e}_\phi]^{\frac{r_3}{r_2}} - f_3 - \hat{d}_3. \end{cases}$$

Theorem 3.2. If the initial states of the attitude tracking error system (2.7) satisfy the constraint

$-\underline{c}_\theta \le e_\theta \le \bar{c}_\theta$, then by choosing appropriate positive constants l_{p1} and l_{d1}, the closed-loop system described by (3.6) is finite-time stable, and the output remains within the predefined constraints for all time.

Proof. The proof proceeds in three steps.

Step 1. Asymptotic stability analysis

Consider the following Lyapunov function candidate for system (3.7):

$$V_1 = l_{p1} V_b(e_\theta) + \frac{|\dot{e}_\theta|^{r_1+1}}{r_1+1},$$

where $V_b(e_\theta)$ is the Barrier Lyapunov Function defined in (3.4).

Differentiating V_1 along the trajectory of system (3.7) yields:

$$\begin{aligned}
\dot{V}_1 &= l_{p1}\lambda(e_\theta)[e_\theta]^{\frac{r_3}{r_1}}\dot{e}_\theta + [\dot{e}_\theta]^{r_1}\ddot{e}_\theta \\
&= l_{p1}\lambda(e_\theta)[e_\theta]^{\frac{r_3}{r_1}}\dot{e}_\theta + [\dot{e}_\theta]^{r_1}\left(-l_{p1}\lambda(e_\theta)[e_\theta]^{\frac{r_3}{r_1}} - l_{d1}[\dot{e}_\theta]^{\frac{r_3}{r_2}}\right) \\
&= -l_{d1}|\dot{e}_\theta|^{\frac{r_3}{r_2}+r_1}.
\end{aligned}$$

It is evident that $\dot{V}_1 \le 0$. When $\dot{V}_1 \equiv 0$, it follows that $\dot{e}_\theta \equiv 0$. According to LaSalle's invariance principle [34], all trajectories of system (3.7) converge to its largest invariant set $M = \{(e_\theta, \dot{e}_\theta) | \dot{e}_\theta \equiv 0\}$. Furthermore, from system (3.7), it can be seen that within this invariant set, $\dot{e}_\theta \equiv 0$ also holds. Consequently, the only equilibrium point within the set M is $(e_\theta, \dot{e}_\theta) = (0, 0)$.

Therefore, the system in (3.7) is asymptotically stable in the region $D \in D_{(-\underline{c}_\theta, \bar{c}_\theta)} \to R$.

Step 2. Finite-time stability analysis

To analyze finite-time stability of (3.7), we rewrite it as:

$$\ddot{e} = -l_{p1}[e_\theta]^{\frac{r_3}{r_1}} - l_{d1}[\dot{e}_\theta]^{\frac{r_3}{r_2}} + \lambda(e_\theta), \tag{3.8}$$

where $p_1(e_\theta) = l_{p1}[e_\theta]^{\frac{r_3}{r_1}}(1-\lambda(e_\theta))$.

To facilitate analysis, the portion of system (3.8) that does not account for uncertainties and disturbances is considered as its nominal system, whose dynamics are described as follows:

$$\ddot{e} = -l_{p1}[e_\theta]^{\frac{r_3}{r_1}} - l_{d1}[\dot{e}_\theta]^{\frac{r_3}{r_2}}. \tag{3.9}$$

For (3.9), choose the Lyapunov function:

$$V_2 = \frac{l_{p1}|e_\theta|^{\frac{r_3}{r_1}+1}}{\frac{r_3}{r_1}+1} + \frac{|\dot{e}_\theta|^{r_1+1}}{r_1+1}.$$

Computing the time derivative of V_2 along the system trajectories yields:

$$\dot{V}_2 = l_{p1}[e_\theta]^{\frac{r_3}{r_1}} + [\dot{e}_\theta]^{r_1}\ddot{e}_\theta$$

$$= l_{p1}[e_\theta]^{\frac{r_3}{r_1}}\dot{e}_\theta + [\dot{e}_\theta]^{r_1}\left(-l_{p1}[e_\theta]^{\frac{r_3}{r_1}} - l_{d1}[\dot{e}_\theta]^{\frac{r_3}{r_2}}\right)$$

$$= -l_{d1}[\dot{e}_\theta]^{\frac{r_3}{r_2}+r_1},$$

where $r = (r_1, r_2)$, It is demonstrated below that system (3.9) is a homogeneous system with respect to $\Delta_\varepsilon^r = (\varepsilon^{r_1}e_\theta, \varepsilon^{r_2}\dot{e}_\theta)$. Let $h(e_\theta) = 1 - \lambda(e_\theta)$. Its Taylor expansion about the origin is

$$h(e_\theta) = \xi\, e_\theta + O(e_\theta),$$

where $\xi = \frac{(r_3+2r_1)(\bar{c}_\theta - \underline{c}_\theta)}{r_1\,\bar{c}_\theta\,\underline{c}_\theta}$.

For any fixed e_θ, consider the limit

$$\lim_{\varepsilon\to 0}\frac{p_1(\varepsilon^{r_1}e_\theta)}{\varepsilon^{r_1+\tau}} = \lim_{\varepsilon\to 0}\frac{l_{p_1}[\varepsilon^{r_1}e_\theta]^{\frac{r_3}{r_1}}h(\varepsilon^{r_1}e_\theta)}{\varepsilon^{r_2+\tau}}$$

$$= \lim_{\varepsilon\to 0}\frac{l_{p_1}\xi[\varepsilon^{r_1}e_\theta]^{\frac{r_3}{r_1}}(\varepsilon^{r_1}e_\theta)}{\varepsilon^{r_3}} + \lim_{\varepsilon\to 0}\frac{l_{p_1}O(\varepsilon^{r_1}e_\theta)[\varepsilon^{r_1}e_\theta]^{\frac{r_3}{r_1}}}{\varepsilon^{r_3}}$$

$$= \lim_{\varepsilon\to 0}O(\varepsilon^{r_1}e_\theta) + \lim_{\varepsilon\to 0}O(\varepsilon^{r_1}e_\theta)$$

$$= 0.$$

From Theorem 3.1, the system in (3.8) is locally finite-time stable, i.e., the closed-loop system (3.7) is finite-time stable. Combining the proofs in Step 1 and Step 2, the following conclusion is obtained according to Theorem 3.1: system (3.8) is finite-time stable over the entire domain Ω.

Step 3. Verification of constraint satisfaction

To verify that the output of system (3.7) remains within the prescribed constrain$-\underline{c}_\theta \le e_\theta \le \bar{c}_\theta$ for all t, let $(e_\theta(t),\ \dot{e}_\theta(t))^T$ denote the solution starting from any initial state $(e_\theta(0), \dot{e}_\theta(0))^T \in D$.

The proof proceeds by contradiction.

Suppose there exists a time instant t_i such that $e_\theta(t_i) \notin (-\underline{c}_\theta, \bar{c}_\theta)$. Either $e_\theta(t_i) > \bar{c}_\theta$ or $e_\theta(t_i) < -\underline{c}_\theta$. Without loss of generality, consider the case where $e_\theta(t_i) > \bar{c}_\theta$.

If $e_\theta(t_i) > \bar{c}_\theta$, according to the Mean Value Theorem [35], there must exist a $t_* \in (t_0,\ t_i)$ such that $e_\theta(t_*) = \bar{c}_\theta$. According to the Barrier Lyapunov Function $V_b(e_\theta)$ in (3.4), it follows that $\lim_{t\to t_*} V_b(e_\theta) = +\infty$.

On the other hand, from Step 1 we have $\dot{V}_1 \le 0$, implying that $V_1(t)$ is non-increasing. Hence

$$k_{p1}V_B\big(e_\theta(t_*)\big) \le V_1(t_*) \le V_1(0) < +\infty.$$

This contradicts $\lim_{t\to t_*^-} V_b(e_\theta) = +\infty$. Therefore, the assumption that $e_\theta(t_i) > \bar{c}_\theta$ is invalid. A similar argument rules out the case $e_\theta(t_i) < -\underline{c}_\theta$.

Hence, for system (3.7) with initial condition satisfying the constraint, we have $-\underline{c}_\theta \le e_\theta(t) \le \bar{c}_\theta$ for all $t \ge 0$.

Remark 3.3. In the absence of output constraint, i.e., $\bar{c}_\theta = \underline{c}_\theta = c = \infty$, the barrier Lyapunov function (3.4) reduces to:

$$\lim_{h\to\infty} V_b(e_\theta) = \frac{|e_\theta|^{\frac{r_3}{r_1}+1}}{\frac{r_3}{r_1}+1}.$$

Moreover, $\lim_{h\to\infty} p_1(e_\theta) = 1$. In this case, the finite-time controller (3.8) transforms into an unconstrained finite-time controller

$$\ddot{e} = -l_{p1}[e_\theta]^{\frac{r_3}{r_1}} - l_{d1}[\dot{e}_\theta].$$

Remark 3.4. The assumption $-\underline{c}_\theta \le e_\theta \le \bar{c}_\theta$ in Theorem 3.2 is a standard prerequisite for the BLF methodology, as the tangent-type BLF tends to infinity at the constraint boundary. Therefore, the proposed controller is inherently a constraint preservation scheme. For initial conditions outside the boundary, a two-stage strategy can be adopted: An unconstrained controller first drives the states into the constraint domain, after which the proposed BLF-based controller is activated.

In the quadrotor UAV system, the actual control inputs are the speeds of the four rotors denoted by ω_1, ω_2, ω_3 and ω_4. These are related to the generalized control commands-total lift u_L and $\tau_\varphi, \tau_\theta, \tau_\psi$ through the following allocation matrix:

$$\begin{bmatrix} \omega_1^2 \\ \omega_2^2 \\ \omega_3^2 \\ \omega_4^2 \end{bmatrix} = \begin{bmatrix} \frac{1}{4} & 0 & -\frac{1}{2} & -\frac{1}{4} \\ \frac{1}{4} & \frac{1}{2} & 0 & \frac{1}{4} \\ \frac{1}{4} & 0 & \frac{1}{2} & -\frac{1}{4} \\ \frac{1}{4} & -\frac{1}{2} & 0 & \frac{1}{4} \end{bmatrix} \begin{bmatrix} \frac{u_L}{k} \\ \frac{\tau_\varphi}{lk} \\ \frac{\tau_\theta}{lk} \\ \frac{\tau_\psi}{b} \end{bmatrix},$$

where the body-frame torque commands $\tau_\varphi, \tau_\theta$ and τ_ψ can be calculated via the transformation $[\tau_\varphi \quad \tau_\theta \quad \tau_\psi]^T = IW^{-1}[\tau_1 \quad \tau_2 \quad \tau_3]^T$. Furthermore, the lift force u_L can be obtained by solving the equilibrium equation (2.4):

$$u_L = \frac{mg}{\cos\varphi \cos\theta}.$$

4. Numerical simulations

4.1. Simulation set up

To verify the effectiveness of the proposed continuous finite-time state feedback control law, numerical simulations are performed for the quadrotor UAV attitude control system. The simulation parameters, including model coefficients, initial attitude states, external disturbances, and controller/observer gains, are summarized as follows:
Model parameters:

$$I_x = I_y = 5.445 \times 10^{-3} kg \cdot m^2, I_z = 1.089 \times 10^{-2} kg \cdot m^2, m = 0.8kg, l = 0.165m,$$

$$b = 2 \times 10^{-6}, k = 2.98 \times 10^{-5}.$$

Initial conditions:

$$\varphi(0) = 0.2, \theta(0) = -0.2, \psi(0) = 0, p(0) = -8, q(0) = 8, r(0) = 0, d_2(0) = 1.$$

External disturbance:

$$d_1 = sin(t),\ d_2 = cos(t),\ d_3 = -sin(t).$$

Attitude angle commands:

$$\varphi^q = -5^\circ + 15^\circ cos\left(\frac{\pi}{2}t\right),\ \theta^q = -10^\circ cos\left(\frac{\pi}{2}t\right),\ \psi^q = 0.$$

Controller parameters, Observer gains:

$$r_1 = 1,\ r_2 = 0.8,\ r_3 = 0.6,\ \gamma = -\frac{2}{11},\ l_{p1} = l_{p2} = l_{p3} = 12, l_{d1} = l_{d2} = l_{d3} = 8, B = 2, k_1 = 15,$$

$$k_2 = 20,\ k_3 = 8,\ k_4 = 2,\ L = 4,\ c_\theta = \frac{\pi}{6},\ r_{ij} = 1 + r_{i,j-1}\gamma, (i = 1, 2, 3, j = 2, \cdots, 5).$$

4.2. Simulation results

4.2.1. Performance verification of the proposed FTSFC

To evaluate the performance of the proposed constrained finite-time control scheme, numerical simulations are carried out for the quadrotor attitude system. The response curves under the designed continuous finite-time state feedback controller are presented in Figures 2–4.

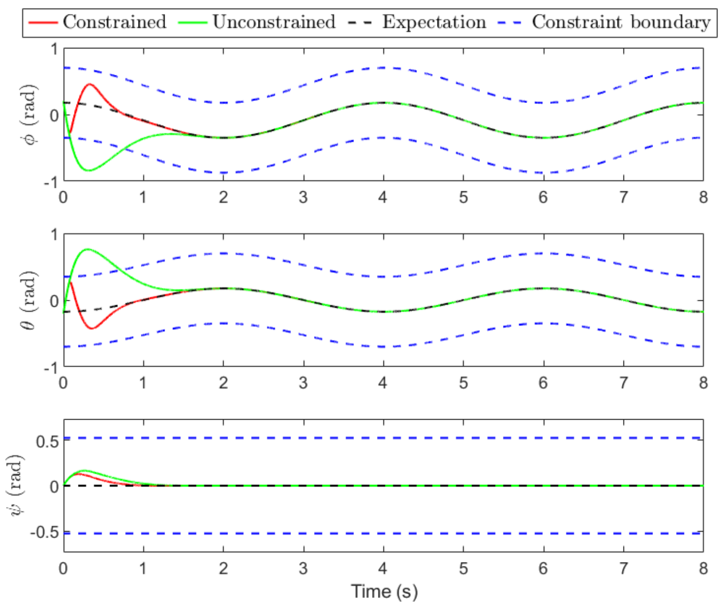

Figure 2. Comparison of attitude tracking performance: constrained vs. unconstrained control.

Figure 2 depicts the attitude angle tracking responses for the three-channel attitude angle tracking commands. Under the proposed constrained controller, the actual angles closely track the time-varying reference commands, with tracking errors strictly maintained within the prescribed bounds thereby validating the efficacy of the barrier Lyapunov function-based constraint handling mechanism. In contrast, the unconstrained controller exhibits noticeable overshoot in the roll and pitch channels, resulting in temporary violations of the allowable limits. This comparison underscores the necessity of incorporating explicit output constraints to ensure tracking accuracy and operational safety.

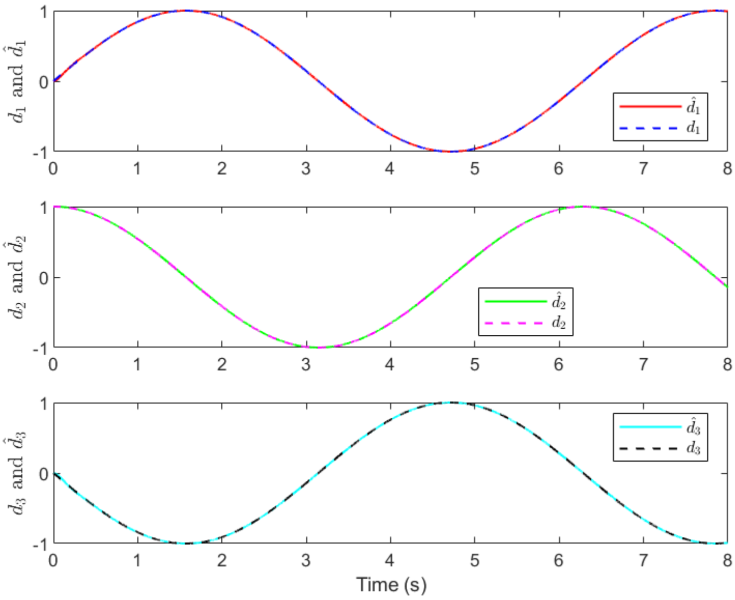

Figure 3. Estimation performance of the disturbance observer for the three channels.

Figure 3 illustrates the estimation performance of the proposed finite-time disturbance observer. The observer rapidly converges to the actual lumped disturbances within a finite time, and the estimation errors remain negligible once steady state is reached. This confirms the observer's capability to accurately reconstruct external disturbances and model uncertainties in real time, thereby providing a reliable foundation for the feed-forward compensation loop and substantially enhancing the system's overall disturbance rejection performance.

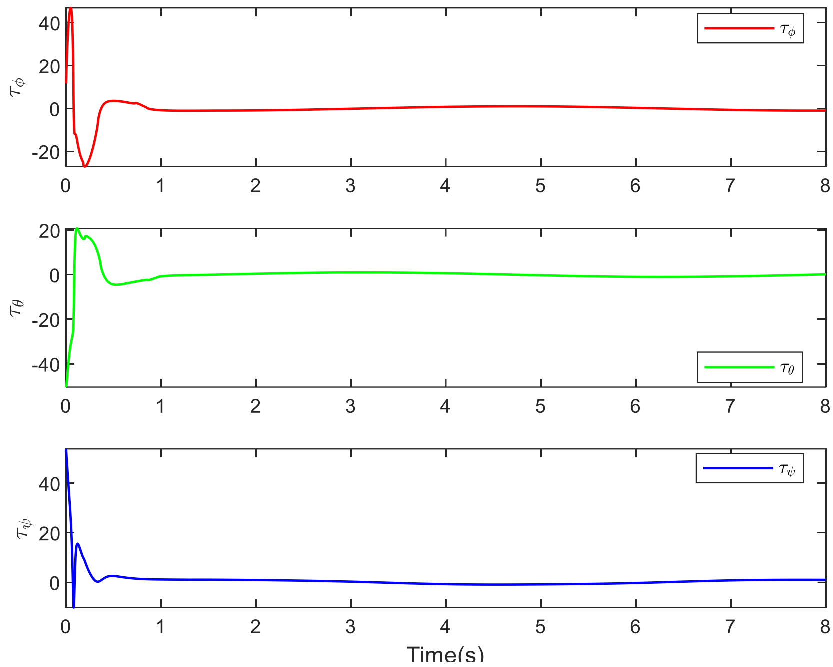

Figure 4. Control torque histories illustrating the adaptive mechanism of the constrained control.

Figure 4 presents the torque curves for the three channels, illustrating the adaptive mechanism inherent to the constrained control strategy. As the attitude angles approach the prescribed boundaries, the control magnitudes increase accordingly this gain adjustment actively prevents constraint violation while avoiding high-frequency oscillations that typically result from abrupt saturation. In non-boundary regions, the control torque exhibits smooth transitions, reflecting a well-balanced trade-off between constraint enforcement and control effort smoothness. Moreover, the coordinated response across channels confirms that the adopted decoupling strategy effectively mitigates inter-channel coupling disturbances.

4.2.2. Sensitivity test involving parameter perturbations

To validate the robustness of the proposed method, three representative test scenarios are considered: inertia perturbation (+20%*J*), strong disturbance (3×d), and the combined worst-case scenario incorporating both effects.

As shown in Figure 5, under the three test scenarios, the proposed FTSFC scheme maintains high-precision attitude tracking, with the tracking errors strictly confined within the prescribed constraints throughout the operation. Figure 6 further demonstrates that the control input adjusts accordingly in response to increased inertia and enhanced wind disturbances, remaining smooth and chattering-free even under the combined worst-case scenario.

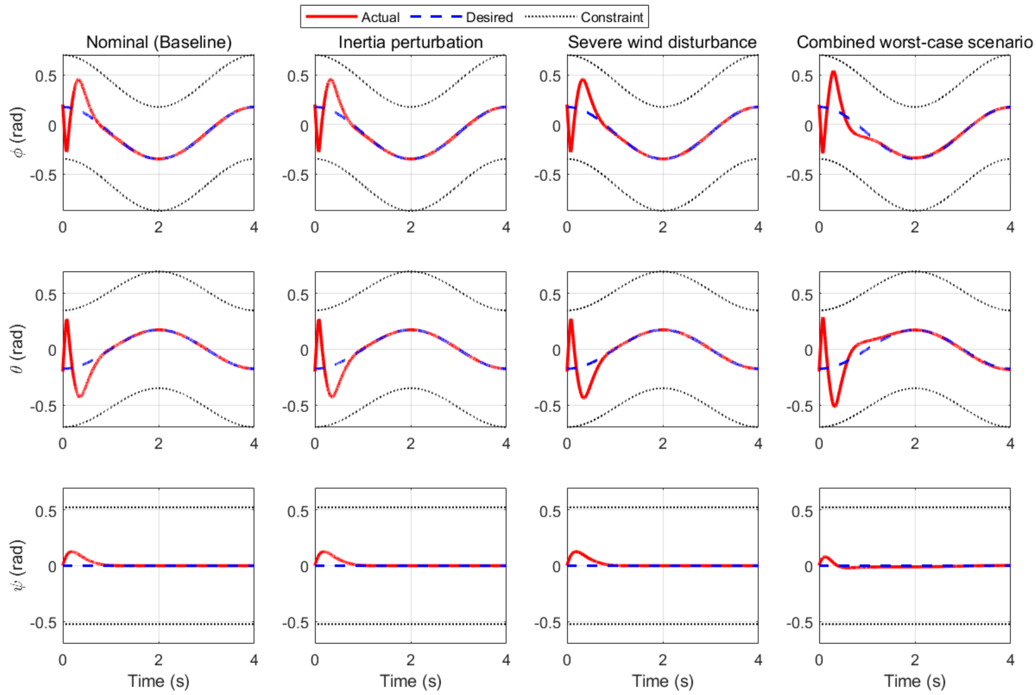

Figure 5. Attitude tracking comparison under parameter perturbation.

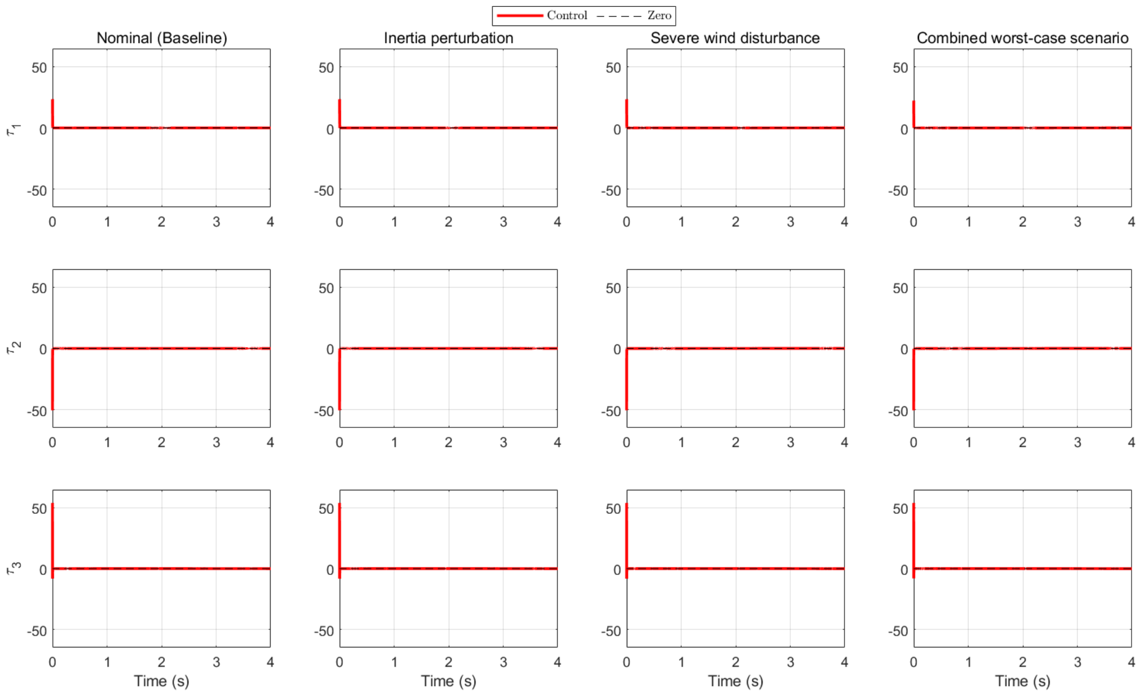

Figure 6. Control input comparison under parameter perturbation.

4.2.3. Comparative study with mainstream advanced algorithms

To validate the superiority of the proposed FTSFC scheme, the compensation function observer based BLF attitude constrained backstepping control (CFO-BLF) strategy in [26] is selected as the benchmark. Figures 7–9 compare the attitude tracking responses, errors, and control torques of the two schemes.

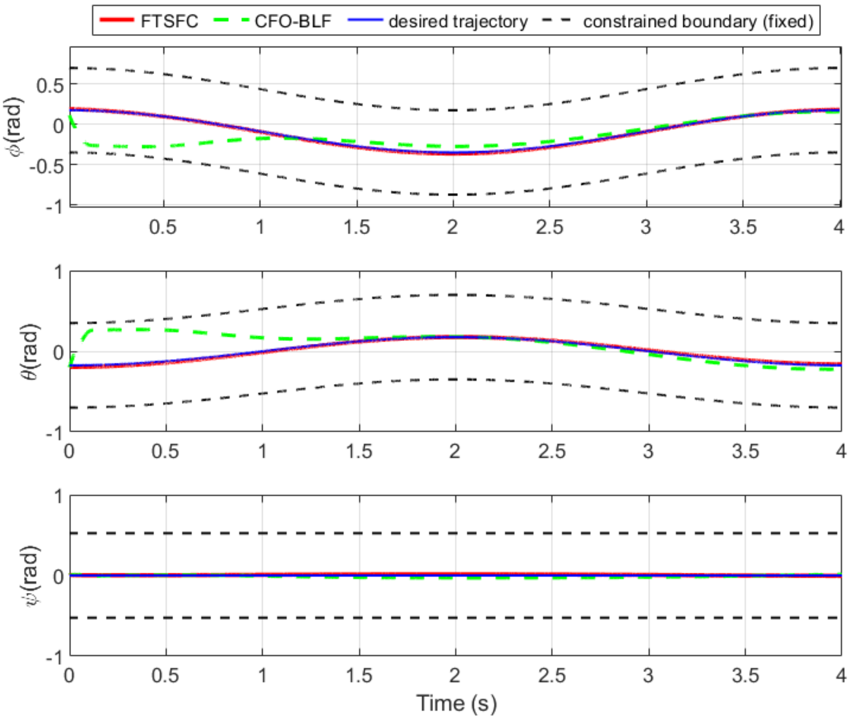

Figure 7. Attitude angle tracking comparison: proposed FTSFC vs CFO-BLF.

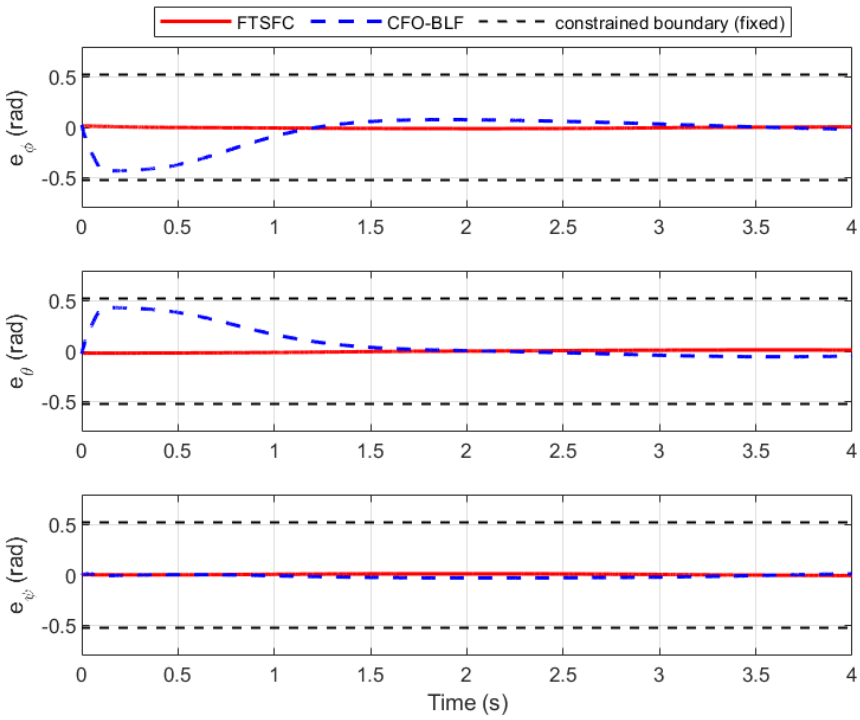

Figure 8. Attitude tracking errors comparison: proposed FTSFC vs CFO-BLF.

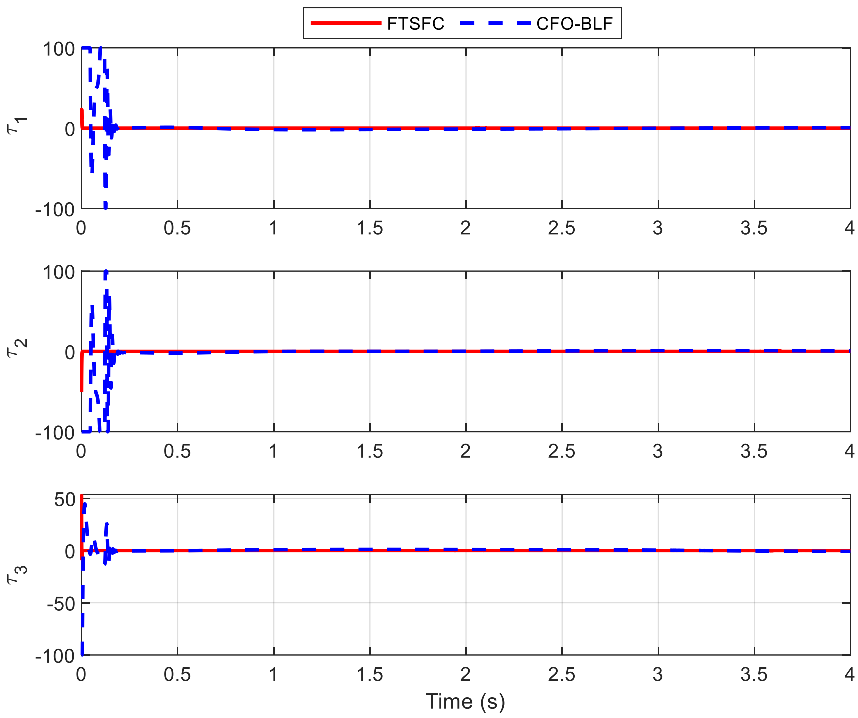

Figure 9. Control input comparison: proposed FTSFC vs CFO-BLF.

As shown in Figure 7, both controllers achieve basic tracking, but CFO-BLF exhibits obvious overshoots and slower transients in roll and pitch channels, while FTSFC provides smoother tracking, faster convergence, and strict constraint satisfaction. Figure 8 demonstrates that FTSFC significantly reduces the maximum tracking errors in all three channels. Figure 9 reveals that FTSFC yields chattering -free control input, whereas CFO-BLF suffers from oscillations during transients, owing to the more accurate and rapid disturbance estimation of the FTDO.

5. Conclusions

In this paper, we investigate the attitude control problem for quadrotor UAVs subject to model uncertainties, external disturbances, and output constraints. A finite-time disturbance observer (FTDO) is designed for rapid estimation of lumped disturbances, and a tangent-type barrier Lyapunov function (BLF) is introduced to develop a continuous finite-time state feedback controller (FTSFC). Theoretical analysis and simulations confirm the scheme's effectiveness in high-precision tracking, constraint satisfaction, and disturbance rejection.

However, several limitations remain. The controller and observer gains lack a systematic tuning procedure, and closed-loop performance is sensitive to these parameters. Moreover, the theoretical analysis assumes bounded lumped disturbances and their derivatives, which may fail under extreme conditions such as wind gusts or actuator failures.

In future work, we will focus on: (i) Systematic sensitivity analysis to guide gain selection; (ii) output-feedback extension via a finite-time state observer using only angle measurements; (iii) adaptive or hybrid disturbance attenuation strategies to relax the boundedness assumption.

The framework also holds promise for extension to multi-agent attitude consensus and impulsive systems. These directions will be pursued in future research.

Author contributions

Huawei Niu: Conceptualization, methodology, formal analysis, validation, writing original draft; Qixun Lan: Supervision, methodology, project administration, funding acquisition, writing-review & editing; Xuehai Wang: Investigation, software, visualization, data curation; Jingjing Mu: Validation, formal analysis, writing review & editing. All authors have read and approved the final version of the manuscript for publication.

Use of Generative-AI tools declaration

The authors declare they have not used Artificial Intelligence (AI) tools in the creation of this article.

Acknowledgments

This work was supported by the National Natural Science Foundation of China (No. 61503122), the Natural Science Foundation of Henan Province (No. 252300420390 and No. 252300421889), and the Scientific Research Incubation Project of Pingdingshan Vocational and Technical College (No. 202202001).

Conflict of interest

The authors declare that they have no competing interests.

References

1. P. Marqués, A. Da Ronch, *Advanced UAV aerodynamics, flight stability and control: Novel concepts, theory and applications*, Wiley, 2017. https://doi.org/10.1002/9781118928691
2. R. Guebsi, S. Mami, K. Chokmani, Drones in precision agriculture: A comprehensive review of applications, technologies, and challenges, *Drones*, **8** (2024), 686. https://doi.org/10.3390/drones8110686
3. Q. Lan, J. Yang, Y. Wang, J. Sun, N. Liu, Finite-time stabilization for a class of high-order uncertain planar systems with an output constraint via output feedback, *Int. J. Syst. Sci.*, **56** (2025), 1943–1958. http://doi.org/10.1080/00207721.2024.2435589
4. I. Lopez-Sanchez, J. Moreno-Valenzuela, PID control of quadrotor UAVs: A survey, *Annu. Rev. Control*, **56** (2023), 100900. https://doi.org/10.1016/j.arcontrol.2023.100900
5. Z. He, W. Gao, X. He, M. Wang, Y. Liu, Y. Song, et al., Fuzzy intelligent control method for improving flight attitude stability of plant protection quadrotor UAV, *Int. J. Agric. Biol. Eng.*, **12** (2019), 110–115. https://doi.org/10.25165/j.ijabe.20191206.5108
6. L. Martins, C. Cardeira, P. Oliveira, Feedback Linearization with zero dynamics stabilization for quadrotor control, *J. Intell. Robot. Syst.*, **101** (2021), 7. https://doi.org/10.1007/s10846-020-01265-2

7. M. A. Lawati, Z. Jiang, A. F. Lynch, Output tracking dynamic feedback linearization of a multirotor suspended load system with disturbance robustness, *J. Intell. Robot. Syst.*, **108** (2023), 82. https://doi.org/10.1007/s10846-023-01904-4
8. N. Vafamand, M. M. Arefi, Robust neural network-based backstepping landing control of quadrotor on moving platform with stochastic noise, *Int. J. Robust Nonlinear Control*, **32** (2022), 2007–2026. https://doi.org/10.1002/rnc.5933
9. W. Sun, L. Wang, Y. Wu, Adaptive dynamic surface fuzzy control for state constrained time-delay nonlinear nonstrict feedback systems with unknown control directions, *IEEE Trans. Syst. Man Cybern. Syst.*, **51** (2020), 7423–7434. https://doi.org/10.1109/TSMC.2020.2969289
10. B. Zhang, J. Zhao, Z. Y. Sun, C. Mu, Adaptive fuzzy switching tracking algorithm for flexible robotic manipulators under stochastic disturbances: Design and experiments, *IEEE Trans. Ind. Electron.*, **73** (2025), 4654–4666. https://doi.org/10.1109/TIE.2025.3607949
11. S. Lian, W. Meng, Z. Lin, K. Shao, J. Zheng, H. Li, Adaptive attitude control of a quadrotor using fast nonsingular terminal sliding mode, *IEEE Trans. Ind. Electron.*, **69** (2022), 1597–1607. https://doi.org/10.1109/tie.2021.3057015
12. M. B. R. Neila, D. Tarak, Adaptive terminal sliding mode control for rigid robotic manipulators, *Int. J. Autom. Comput.*, **8** (2011), 215–220. https://doi.org/10.1007/s11633-011-0576-2
13. Q. Lan, J. Yang, J. Sun, Y. Wang, N. Liu, Robust finite-time output feedback stabilization for a class of uncertain planar systems with asymmetric output constraints, *Int. J. Control*, **98** (2024), 1612–1625. https://doi.org/10.1080/00207179.2024.2411599
14. M. Chen, S. X. Xiong, Q. X. Wu, Tracking flight control of quadrotor based on disturbance observer, *IEEE Trans. Syst. Man Cybern. Syst.*, **51** (2021), 1414–1423. https://doi.org/10.1109/TSMC.2019.2896891
15. Q. Lan, P. Yue, N. Liu, J. W. Sun, S. Liu, Finite-time position tracking control for magnetic levitation systems with suspension air-gap constraints, *Appl. Math. Model.*, **148** (2025), 116258. https://doi.org/10.1016/j.apm.2025.116258
16. X. B. Lin, Y. Yu, C. Sun, A decoupling control for quadrotor UAV using dynamic surface control and sliding mode disturbance observer, *Nonlinear Dyn.*, **97** (2019), 781–795. https://doi.org/10.1007/s11071-019-05013-6
17. A. Khadhraoui, A. Zouaoui, M. Saad, Barrier Lyapunov function and adaptive backstepping-based control of a quadrotor UAV, *Robotica*, **41** (2023), 2941–2963. https://doi.org/10.1017/s0263574723000735
18. F. Wang, H. M. Gao, K. Wang, C. Zhou, Q. Zong, C. Hua, Disturbance observer-based finite-time control design for a quadrotor UAV with external disturbance, *IEEE Trans. Aerosp. Electron. Syst.*, **57** (2021), 834–847. https://doi.org/10.3390/electronics9101624
19. K. Liu, R. Wang, X. Wang, X. Wang, Anti-saturation adaptive finite-time neural network based fault-tolerant tracking control for a quadrotor UAV with external disturbances, *Aerosp. Sci. Technol.*, **115** (2021), 106790. https://doi.org/10.1016/j.ast.2021.106790
20. J. Zhao, L. Qiu, Z. Y. Sun, H. Yan, W. Zhang, A new approach to designated-time stabilizing strategy of stochastic nonlinear systems and its application to mass-spring mechanical system. transactions on systems, *IEEE Trans. Syst. Man Cybern. Syst.*, **56** (2026), 1151–1164. https://doi.org/10.1109/TSMC.2025.3647491
21. T. Xiao, J. Guo, J. Chen, D. Sun, D. Li, J. Xiang, Tracking control of quadrotor UAVs with prescribed performance and prescribed-time convergence under arbitrary initial conditions, *Electronics*, **15** (2026), 408. https://doi.org/10.3390/electronics15020408

22. M. Tian, N. Wang, Z. Wang, Z. Fu, F. Tao, Prescribed-time fault-tolerant tracking control for quadrotor UAV with guaranteed performance, *Aerosp. Sci. Technol.*, **161** (2025), 110162. https://doi.org/10.1016/j.ast.2025.110162
23. X. Wang, M. Chen, Y Gai, Y. Sun, H. Wang, A novel prescribed finite-time attitude tracking control of quadrotor UAVs, In: *2024 7th international symposium on autonomous systems (ISAS)*, 2024, 1–6. https://doi.org/10.1109/isas61044.2024.10552504
24. C. Zhang, J. Wang, S. Fan, Y. Chen, UAV guaranteed performance anti-saturation fast super-twisting sliding mode attitude tracking control, *Nonlinear Dyn.*, **113** (2025), 13261–13276. https://doi.org/10.1007/s11071-024-10845-y
25. S. Vutukuri, R. Padhi, Robust adaptive predefined time prescribed performance attitude control for spacecraft, *Control Eng. Pract.*, **157** (2025), 106271. https://doi.org/10.1016/j.conengprac.2025.106271
26. G. Qi, K. Li, K. Wang, Attitude-constrained control of quadrotor UAV based on compensation function observer, *J. Jilin Univ.*, **53** (2023), 853–862. https://doi.org/10.13229/j.cnki.jdxbgxb.20220612
27. B. Ma, Z. Liu, W. Zhao, J. Yuan, H. Long, X. Wang, et al., Target tracking control of UAV through deep reinforcement learning, *IEEE Trans. Intell. Transp. Syst.*, **24** (2023), 5983–6000. https://doi.org/10.1109/tits.2023.3249900
28. X. B. Lin, J. Liu, Y. Yu, C. Sun, Event-triggered reinforcement learning control for the quadrotor UAV with actuator saturation, *Neurocomputing*, **415** (2020), 135–145. https://doi.org/10.1016/j.neucom.2020.07.042
29. Y. Luo, H. Yu, H. Zhang, Y. Zhou, A novel Newton–Euler method-based nonlinear anti-swing control for a quadrotor UAV carrying a slung load, *IEEE Trans. Syst. Cybern. Syst.*, **54** (2024), 2266–2275. https://doi.org/10.1109/TSMC.2023.3342027
30. C. Zhou, X. Wang, J. Yang, H. Yu, S. Li, Robust safe motion control for compliantly actuate robots via disturbance observers, *IEEE/ASME Trans. Mechatron*, **29** (2024), 2794–2802. https://doi.org/10.1109/TMECH.2024.3399842
31. H. Wang, Y. Zhang, Z. Zhao, X. Tang, J. Yang, I. M. Chen, Finite-time disturbance observer based trajectory tracking control for flexible-joint robots, *Nonlinear Dyn.*, **106** (2021) 459–471. https://doi.org/10.1007/s11071-021-06868-4
32. J. Li, C. Qian, M. Frye, A dual-observer design for global output feedback stabilization of nonlinear systems with low-order and high-order nonlinearities, *Int. J. Robust Nonlinear Control*, **19** (2009), 1697–1720. https://doi.org/10.1002/rnc.1401
33. Q. Liang, Q. Lan, S. Liu, P. Yue, P. Zhao, Finite-time disturbance observer-based finite-time robust attitude control for quadrotor UAVs, In: *2025 40th Youth academic annual conference of Chinese association of automation (YAC)*, 2025, 1190–1195. https://doi.org/10.1109/YAC66630.2025.11149750
34. D. Shevitz, B. Paden, Lyapunov stability theory of nonsmooth systems, *IEEE Trans. Autom. Control*, **39** (1994), 1910–1914. https://doi.org/10.1109/9.317122
35. J. Stewart, D. Clegg, S. Watson, *Calculus: Early transcendentals*, Cengage, 2021.

Supplementary

List of principal symbols.

Symbol	Description
$\Theta = [\varphi, \theta, \psi]$	Attitude Euler angles vector (roll, pitch, yaw)
$\Theta^q = [\varphi^q, \theta^q, \psi^q]$	Desired attitude angles
$e_\Theta = [e_\varphi, e_\theta, e_\psi]$	Attitude tracking error vector
$\tau_d = [\tau_{d_\varphi}, \tau_{d_\theta}, \tau_{d_\psi},]$	External disturbance torque vector
$\omega_1, \omega_2, \omega_3, \omega_4$	Rotational speeds of the four rotors
$\Omega = [p, q, r]^T$	Angular velocity vector in body frame
$\Omega_\times = [p, q, r]^T$	kew-symmetric matrix
W	Attitude kinematics matrix
$I = diag[I_x, I_y, I_z]$	Inertia matrix of quadrotor
$\tau = [\tau_1, \tau_2, \tau_3]$	Control inputs vector
$\tau_u = [\tau_\varphi, \tau_\theta, \tau_\psi]^T$	Control torque vector
$f = [f_1, f_2, f_3]^T$	nonlinear dynamics vector
$d = [d_1, d_2, d_3]$	Lumped disturbance vector (includes external disturbances and model uncertainties)
$\hat{d}_i$	Estimate of the lumped disturbance from the FTDO
e_1, e_2, e_3	Estimation errors of the finite-time disturbance observer
$k_{i1}, k_{i2}, k_{i3}, k_{i4}$	Positive definite constants (controller gains)
l_{pi}, l_{di}	Positive definite constants (controller gains)
$\lambda_1, \lambda_2, \lambda_3$	Observer gains for the FTDO
$r_{i,j} (i, j = 1, \cdots, n)$	Recursively defined exponents for the FTDO (odd/even integers)
L	Observer gains

Symbol	Description
$l_i(i=1,\cdots,n)$	Observer coefficients based on Lemma 1
m	Mass of the quadrotor UAV
g	Gravitational acceleration
u_L	Total lift force generated along the body z-axis
l	Arm length from rotor center to UAV's center of mass
k	the thrust coefficient
b	the torque coefficient
$V_b(e_\theta)$, V_1, V_2	Barrier Lyapunov Function (BLF) of tangent type
$\underline{c}_\theta, \bar{c}_\theta$	Constraints
$[e_\theta]^\alpha$	$\|e_\theta\|^\alpha sign(e_\theta)$
$sat(\cdot)$	Saturation function used in the FTDO for practical implementation
D	Domain of attraction / region where the system is stable